Post-print of Martín-Gómez, Paula et al. "Isotope-Ratio Infrared Spectroscopy: a reliable tool for the investigation of plant-water sources?" in New Phytologist, Vol. 207, Issue 3 (August 2015), p. 914-927. Wiley. The final version is available at DOI 10.1111/nph.13376

Isotope-Ratio Infrared Spectroscopy: a reliable tool for the investigation of plant-water sources?

Martín-Gómez, Paula[1]; Barbeta, Adrià[2,3]; Voltas, Jordi[1]; Peñuelas, Josep[2,3]; Dennis, Kate[4]; Palacio, Sara[5]; Dawson, Todd E[6]; Ferrio, Juan Pedro[1*]

[1]Dept. Crop and Forest Sciences-AGROTECNIO Center, Universitat de Lleida, E-25198 Lleida, Spain; [2]CSIC, Global Ecology Unit CREAF-CSIC-UAB, E-08193 Cerdanyola del Valles (Catalonia), Spain; [3]CREAF, E-08193 Cerdanyola del Vallès (Catalonia), Spain; [4]Product Manager for Isotopic Water, Picarro Inc., Santa Clara, California 95054, USA; [5]Instituto Pirenaico de Ecología (IPE-CSIC), E-22700 Jaca, Spain; [6]Department of Integrative Biology, University of California, Berkeley, California 94720 USA

*Corresponding author:
Juan Pedro Ferrio
Dept. of Crop and Forest Sciences-AGROTECNIO Center
Universitat de Lleida
Avda. Rovira Roure 191, E-25198 Lleida (Spain)
Phone: +34 973 702511
e-mail: pitter.ferrio@pvcf.udl.es

Total word count (excluding summary, references and legends):	5795	Nº of Figures:	6 (Figs. 1,4,5,6 in colour)
Summary:	199	Nº of Tables:	4
Introduction:	853	Nº of Supporting Information Files:	0
Materials and methods:	1847		
Results:	1394		
Discussion:	1579		
Acknowledgments:	115		

SUMMARY

- Stable isotopes are extensively used as tracers for the study of plant-water sources. Isotope-ratio infrared spectroscopy (IRIS) offers a cheaper alternative to isotope-ratio mass spectroscopy (IRMS), but its use in plant and soil water is limited by the spectral interference caused by organic contaminants. Here, we examine two approaches to cope with contaminated samples in IRIS: on-line oxidation of organic compounds (MCM) and post-processing correction.
- We assessed these methods compared to IRMS across 136 samples of xylem and soil water and a set of ethanol- and methanol-water mixtures.
- A post-processing correction improved significantly IRIS accuracy in both natural samples and alcohol dilutions, being effective with concentrations up to 8% of ethanol and 0.4% of methanol. MCM outperformed the post-processing correction in removing methanol interference, but was not effective for high concentrations of ethanol.
- By using both approaches IRIS can overcome with reasonable accuracy the analytical uncertainties associated to most organic contaminants found in soil and xylem water. We recommend the post-processing correction as the first choice for the analysis of samples of unknown contamination. Nevertheless, MCM can be more effective for samples containing contaminants responsible of strong spectral interferences from small concentrations, such as methanol.

Keywords:

CRDS, ecohydrology, $\delta^{18}O$, $\delta^{2}H$, IRIS, IRMS, soil, xylem

INTRODUCTION

The stable isotope composition of oxygen ($\delta^{18}O$) and hydrogen ($\delta^{2}H$) in xylem water is widely used as a tracer for the study of plants and fungi water uptake and redistribution (Ehleringer & Dawson, 1992; Dawson, 1996; Warren *et al.*, 2008; Lilleskov *et al.*, 2009; Dawson & Simonin, 2011; Moreno-Gutiérrez *et al.*, 2012; Prieto *et al.*, 2012; Palacio *et al.*, 2014a; Treydte *et al.*, 2014). Recently, the widespread use of isotope-ratio mass spectrometry (IRMS) technology for measuring water isotopes has been challenged by the development of isotope-ratio infrared spectroscopy (IRIS). IRIS methods provide isotopic compositions of water samples by spectroscopy, taking advantage of the different absorption spectra of water isotopologues in the gaseous phase (Lis *et al.*, 2008; Gupta *et al.*, 2009). This allows the simultaneous measurement of $^{1}H_{2}{}^{16}O$, $^{1}H_{2}{}^{18}O$, and $^{1}H^{2}H^{16}O$ with an accuracy comparable to IRMS, at least when analysing pure water (Lis *et al.*, 2008; Brand *et al.*, 2009; Gupta *et al.*, 2009; West *et al.*, 2010, 2011). IRIS, unlike IRMS, does not need the prior chemical equilibration or conversion into elemental constituents that often limits precision (Brand *et al.*, 2009; Schultz *et al.*, 2011; Schmidt *et al.*, 2012). IRIS also offers other advantages such as lower cost, easier installation and maintenance, and higher portability (Brand *et al.*, 2009; Gupta *et al.*, 2009; Berman *et al.*, 2009; West *et al.*, 2010; Johnson *et al.*, 2011; Schmidt *et al.*, 2012).

However, some organic contaminants significantly interfere with the water-isotope spectrum in IRIS analyses (Brand *et al.*, 2009; West *et al.*, 2010, 2011). Organics are broadly found together with water in plant and soil samples, and cryogenic distillation, which is the most common method for extracting water from plant and soil matrices, frequently co-distils them. The magnitude of the error caused by organic interference is not only proportional to the amount of contaminant, but also depends on its spectral properties; for some compounds, the associated analytical errors may become unacceptable starting at very small concentrations (e.g. <0.1% for methanol (Brand *et al.*, 2009)). In contrast, the magnitude of the errors associated with contaminants in IRMS depends on the mass-balance contribution of the contaminant to the pool of H and O atoms in the sample. Hence, substantial errors can only be expected for IRMS if the concentration of the contaminant is high and/or the isotopic composition of the organic compound differs strongly from that of water (Brand *et al.*, 2009; West *et al.*, 2010).

IRIS manufacturers have developed software applications that can identify and flag potentially contaminated samples (e.g. Spectral Contamination Identifier, Los Gatos Research, Inc., Mountain View, CA; ChemCorrect™, Picarro Inc., Santa Clara, CA). In the case of Picarro's, firstly ChemCorrect™ compares the measured spectral profile of the sample with that of small molecules such as methane and methanol contained in its library. If the features match, the compound concentration is calculated. Afterwards, the software uses a set of quantitative spectral indicators (mainly spectral baseline and slope) to generate information of larger organics, such as ethanol and other alcohols, included in a 'C_{2+} alcohols' pool (Picarro, 2010; Richman *et al.*, 2010). Thus, a set of organic-corrected spectra is currently available for post-processing correction in the raw data files of L2110-*i* and L2120-*i* models. Later Picarro models (L2130-*i* and L2140-*i* analysers) do not include this information in the raw data files, but a new post-fit correction for these models is expected to be released in the future (Picarro development team, personal communication). The protocol for deriving corrected isotopic values from the spectral data is available for registered users in the Picarro forum. However, it has not been extensively validated due to limited accessibility and, therefore, not widely used to date.

More recently, Picarro Inc. has developed the Micro-Combustion Module™ (MCM) to remove organic compounds interfering with pure water; the MCM uses high-temperature oxidation to eliminate problematic contaminants in the water sample (Picarro, 2012; Saad *et al.*, 2013). Briefly, once a sample is evaporated the entire gaseous phase is swept in a carrier gas across the heated metal catalyst in which oxidation efficiently converts the organics into minute quantities of CO_2 and nascent water. This procedure is expected to eliminate most common alcohols and other plant contaminants of low molecular weight, including multicomponent mixtures of alcohols and terpenes, and green-leaf volatiles. Its optimal efficacy is claimed to be achieved for samples containing total organics at concentrations lower than 0.5%, with a complete elimination for higher concentrations not entirely guaranteed. However, the effectiveness of the MCM pre-treatment and post-processing corrections in soil and xylem samples still requires full testing.

We present here the first evaluation of the performance of MCM using an array of soil and xylem samples from a wide range of sites and species; these results are compared with standard IRIS analyses without the MCM installed. We also present the first validation of a post-processing method, based on ChemCorrect™ post-fit spectral

information, to reduce the effects of organic contamination on water isotopic analysis. Both MCM and post-processed values are validated in field-collected samples against IRMS, and further tested by using a set of standard dilutions of two representative contaminants (methanol, MeOH, and ethanol, EtOH).

MATERIALS AND METHODS

Sample collection and water extraction

We tested 136 samples from 26 species (xylem samples) and 8 sites (soil samples). The samples were collected from a range of Mediterranean-type ecosystems in Spain and the USA (Table 1) following the same standard procedure (Moisture Isotopes in the Biosphere and Atmosphere -MIBA- protocol from International Atomic Energy Agency -IAEA-, available at http://www-naweb.iaea.org/napc/ih/IHS_resources_miba.html). The species belonged to 13 families, which were subsequently used as main taxonomic units. Sunlit twigs were harvested near midday, bark and phloem were removed, and the xylem was immediately sealed in glass vials (air-tight tubes, Duran GL-18). Soil samples from different depths were simultaneously collected and were also rapidly sealed in glass vials. The samples were placed on dry ice in the field and kept frozen until processing.

The extraction of water from the soil and xylem samples was performed by cryogenic vacuum distillation (Dawson & Ehleringer, 1993). Samples from the Iberian Peninsula were processed at the Dept. of Crop and Forest Sciences, Universitat de Lleida (Spain). The extraction system consisted of 10 sample tubes connected with Ultra-Torr™ fittings (Swagelok Company, Solon, Ohio, USA) to 10 U-shaped collection tubes specifically designed for this system. The sample tubes were submerged in mineral oil at a constant temperature (110-120ºC) to evaporate water and the U-tubes were cooled with liquid nitrogen to condense the water vapour. The extraction system was connected to a vacuum pump (model RV3; Edwards, Bolton, UK) to guarantee the flow of water vapour from the sample tubes to the collection tubes and to prevent contamination with atmospheric water vapour. The entire system maintained constant vacuum pressures of *ca.* 10^{-2} mbar. Distillation of sample collected in the USA was conducted at the Center for Stable Isotope Biogeochemistry at the University of California, Berkeley, CA, USA, using the same procedure but with a slightly different design (Goldsmith *et al.*, 2012).

Ethanol- and methanol-water mixtures

To determine the influence that organic contaminants may have on the analysis of isotope ratios of water using either IRIS or IRMS, we prepared a set of mixtures with different concentrations of two organic compounds, EtOH and MeOH, representative of

broadband (baseline) and narrowband spectral interference, respectively (Schultz *et al.*, 2011; Leen *et al.*, 2012). The mixtures were used as known "reference" samples by mixing EtOH or MeOH with water of known isotopic composition ($\delta^{18}O$ = -9.48‰, $\delta^{2}H$ = -65.05‰). EtOH was mixed with water at concentrations of 0.5, 1, 2, 4, and 8% (vol./vol.) and MeOH at 0.1, 0.2, 0.4, 0.8, and 1.6% (vol./vol.). An additional set of dilutions was prepared combining both compounds at two concentrations (2 and 8% EtOH with 0.4 and 1.6% MeOH). The same set of mixtures was used to fit linear regressions for 1) predicting the error associated with varying contaminant concentration, as proposed in earlier studies (Brand *et al.*, 2009; Schultz *et al.*, 2011; Leen *et al.*, 2012), and 2) estimating MeOH-equivalent and EtOH-equivalent concentrations in natural samples. For this purpose, we took the unitless contaminant levels determined by ChemCorrect™ and identified as 'ORGANIC_MEOH_AMPL' (for MeOH) and 'ORGANIC_BASE' (for EtOH) in the raw output files (.csv).

Isotopic analyses

We analysed the water isotopes of the xylem and soil samples and of the standard dilutions by IRMS and IRIS. Isotopic ratios were expressed relative to international standard (VSMOW, Vienna Standard Mean Ocean Water) in per mil notation (‰) (i.e. isotopic composition):

$$\delta^{18}O \text{ or } \delta^{2}H = \left(R_{sample}/R_{standard} - 1\right) \times 1000 \quad (1)$$

where R_{sample} and $R_{standard}$ are the heavy to light isotopic ratios ($^{2}H/H$ and $^{18}O/^{16}O$) of the sample and the standard, respectively.

IRMS methods

We used three different methods for IRMS analysis: (1) $\delta^{18}O$ and $\delta^{2}H$ by high temperature pyrolysis (labelled as TCEA), conducted at the Paul Scherrer Institute (Villigen, Switzerland); (2) $\delta^{18}O$ by CO_2 headspace equilibration using a GasBench II system (labelled as GB; Thermo Finnigan, Bremen); and (3) $\delta^{2}H$ by reduction over chromium using an H/Device (labelled as HDEV; Thermo Finnigan, Bremen). The latter two methods were applied at the Center for Stable Isotope Biogeochemistry (Berkeley, CA, USA). For determining $\delta^{18}O$ and $\delta^{2}H$ by high-temperature pyrolysis (1),

a 0.6 µl aliquot of the water sample was injected into a High Temperature Combustion Elemental Analyzer (TC/EA, Thermo Finnigan, Bremen). The water was reduced at 1450ºC on glassy carbon to H_2 and CO, and these components were then carried in a helium stream to the mass spectrometer (Delta plus XP, Thermo Finnigan, Bremen). The hydrogen isotope ratio was determined from the $^{2}H/^{1}H$ ratio of the H_2 molecule, and the oxygen isotope ratio was determined from the $^{12}C^{18}O/^{12}C^{16}O$ ratio of the CO molecule. The precision of this method (1σ standard error of replicates of reference samples) was estimated to be <0.2‰ for $\delta^{18}O$ and <1.0‰ for $\delta^{2}H$. In the GasBench method (2), water samples were equilibrated with a 0.2% CO_2 headspace in Helium for 48 h at 21-23ºC and later inserted into the GasBench II system connected to the Delta Plus XL mass spectrometer, which measured the $^{18}O/^{16}O$ ratio from the CO_2. The precision was about 0.12‰ for $\delta^{18}O$. In the chromium combustion method (3), microlitre quantities of water were injected into the H/Device and reduced to H_2 gas. The $^{2}H/H$ ratio of this gas was measured by the coupled Delta Plus mass spectrometer. The precision for this method was about 0.80‰ for $\delta^{2}H$.

IRIS methods

The IRIS analyses used L2120-*i* and L1102-*i* isotopic water analysers (Picarro Inc., Sunnyvale, CA, USA) available at the Serveis Científico-Tècnics of the Universitat de Lleida (Lleida, Spain) and at the Center for Stable Isotope Biogeochemistry of the University of California (Berkeley, USA) respectively. The L2120-*i* was coupled to an A0211 high-precision vaporiser, and the L1102-*i* was coupled to a V1102-*i* vaporisation module. One microlitre of water was injected into a vaporisation chamber, and the vapour was then passed into an infrared absorbance cavity. The hydrogen and oxygen isotope ratios were calculated by measuring the decay time of laser light at specific wavelengths on the cavity and by reference to the absorption peaks of the three most abundant isotopologues of water ($H_2{}^{16}O$, $HD^{16}O$, and $H_2{}^{18}O$) (Cavity Ring-Down Spectroscopy – CRDS (Gupta *et al.*, 2009)). The estimated precision for the L2120-*i*, based on the repeated analysis of 4 reference water samples was 0.10‰ and 0.40‰, for $\delta^{18}O$ and $\delta^{2}H$, respectively. The long-term external precision for the L1102-*i* is 0.14‰ for $\delta^{18}O$ and 1.0‰ for $\delta^{2}H$.

Micro-Combustion Module

After the analysis of water samples with both L2120-*i* and L1102-*i* set with default settings, the MCM was installed to reanalyse a subset of 79 samples representing most plant species and soil samples. The MCM was integrated in-line between the Picarro vaporiser and the L2120-*i* water-isotope analyser at the Serveis Científico-Tècnics of the Universitat de Lleida. Samples with a small amount of water available after long-term storage were discarded to avoid potential fractionation effects.

Spectral analysis of IRIS data: ChemCorrect™ and post-processing correction

A first quality assessment of the spectral IRIS data was made by running the PostProcess ChemCorrect™, version 1.2.0 (Picarro Inc., Santa Clara, CA) with "chemcorrect_inst avg_orgeval_06.csv" instruction file. This software does not perform corrections on contaminated data but assigns metrics describing the magnitude of the contamination and its potential source. The software also includes flagging indicating the degree of potential contamination by a colour code: green for uncontaminated samples, yellow for possibly contaminated samples (i.e. warranting further attention), and red for very contaminated samples (i.e. designating unreliable results).

As described in Picarro's forum (link only available for registered users: http://www.picarro.com/community/picarro_community/applying_corrections_to_contaminated_water_isotope_measurements_using_ch#comment-964) the raw output files (.csv extension) from the Picarro analysers also provide values of $H_2{}^{18}O$, $HD^{16}O$, and $H_2{}^{16}O$ peaks filtered by the spectral features of organic compounds (columns 'ORGANIC_77', 'ORGANIC_82' and 'SPLINEMAX', respectively). The values of the filtered peaks can be converted to organic-corrected $\delta^{18}O$ and $\delta^{2}H$ by applying unit-specific factory calibration settings (*slope* and *offset*) as:

$$\delta^{2}H = slope \times \left(HD^{16}O / H_2{}^{16}O\right) + offset \quad (2)$$

$$\delta^{18}O = slope \times \left(H_2{}^{18}O / H_2{}^{16}O\right) + offset \quad (3)$$

The values for *slope* and *offset* can be found in the file "Picarrocrds.ini" for Picarro L11xx-*i* units, and the files "InstrCal_Air.ini" and "InstrCal_N2.ini" (measuring in air and N_2, respectively) for L21xx-*i* units. After including these formulae in a custom-made Excel spreadsheet, we ended up with two columns with the pre-existing

uncorrected values (labelled as 'd(18_16)Mean' and 'd(D_H)Mean' in the original .csv file), plus two new columns of post-processed values. In both cases, calibration was then performed by fitting a linear regression to two sets of three internal laboratory standards included in each batch, using the same custom-made Excel spreadsheet. It should be noted that we did not use the results from the calibration procedure included in ChemCorrect™, since this could only be applied to the original, uncorrected values.

Data analysis

Differences between IRMS, uncorrected IRIS and post-processed IRIS measurements were estimated using mixed models based on Restricted Maximum Likelihood (REML) estimations for both $\delta^{18}O$ and $\delta^{2}H$ ($\alpha = 0.05$). Type of analysis (IRMS, IRIS uncorrected, IRIS post-processed, MCM and MCM plus post-processing), type of sample (plant family or soil) and their interaction were considered as fixed factors, while species within family and sample ID were taken as random factors. The effectiveness of the different methods in field-collected samples was assessed by the determination coefficient (R^2) of the linear regression between IRIS and IRMS values, and the root mean square error (RMSE), calculated as follows:

$$\mathrm{RMSE} = \sqrt{\left(Y_{\mathrm{IRIS}} - Y_{\mathrm{IRMS}}\right)^2 / N} \qquad (4)$$

Where Y_{IRIS} and Y_{IRMS} stand for measured IRIS and IRMS, respectively, and N is the number of samples. Hence, we assumed that IRMS provided "true" values and also uniform results across IRMS methods. Indeed, a previous study (West *et al.*, 2010) reported very consistent isotopic ratios among IRMS methods (HDEV, TCEA, and GB), with discrepancies lower than the range of long-term instrument precision. To assess the capacity of ChemCorrect™ to flag contaminated samples and to better understand the limitations of each method, we plotted the differences between IRIS and IRMS values by plant family and ChemCorrect™ category.

For the batch of standard dilutions of MeOH and EtOH, the error was directly calculated as the difference between the measured value of each dilution (both IRIS and IRMS) and that of pure water analysed by IRMS. As a broad quality threshold for method comparison, we adopted the values of the maximum accepted bias (MAB)

applied in the most recent proficiency test for the analysis of water isotopes coordinated by the Isotope Hydrology Section of the IAEA (±0.8‰ and ±6‰ for $\delta^{18}O$ and $\delta^{2}H$, respectively; http://nucleus.iaea.org/rpst/ReferenceProducts/Proficiency_Tests/IAEA-TEL-2011-01/index.htm, M. Groening, pers. comm.). Other studies have proposed narrower limits for accuracy on hydrological studies (e.g. ±0.2‰ for $\delta^{18}O$ and ±2‰ for $\delta^{2}H$, as used in the IAEA inter-laboratory test WICO2011, see Wassenaar *et al.*, 2012 or ±0.15‰ for $\delta^{18}O$ and ±1‰ for $\delta^{2}H$ in Wassenaar *et al.*, 2014). However, since in our study we compared different methods and different laboratories among them, and not against a reference value, we considered more informative to use a broader threshold as primary assessment. In any case, in order to overcome the limitations associated to the use of arbitrary thresholds to identify a proper methodology we also assessed the distribution of errors among the samples using a histogram with 0.2‰ and 2‰ classes for $\delta^{18}O$ and $\delta^{2}H$, respectively. Statistical analyses were performed with JMP Pro 11 (SAS Inc., Cary, NC, USA).

RESULTS

Effect of contaminants on water isotopic composition and correction methods: ethanol- and methanol-water mixtures

Table 2 shows the range of deviations of IRIS and IRMS values from IRMS analysis of pure water (used as reference value) for the set of mixtures. The errors associated with mixtures at different MeOH and EtOH concentrations are shown in Fig. 1. MeOH/water mixtures analysed by IRIS differed substantially from the reference value starting at the lowest contaminant concentration (0.1% MeOH), with maximum discrepancies between the uncorrected IRIS and the IRMS reference value as large as -142.96 and -1077‰ for $\delta^{18}O$ and $\delta^{2}H$, respectively. In contrast, EtOH did not interfere as strongly with pure water, even at very high concentrations (up to 8%). Maximum differences were -0.39‰ for $\delta^{18}O$ and -10.76‰ for $\delta^{2}H$. The error exceeded the established maximum bias for $\delta^{2}H$ only at concentrations of 8%. Similarly, the interferences caused by MeOH and EtOH mixtures on water isotopic signatures were mostly due to MeOH, as any particular combination of EtOH and MeOH produced a deviation in isotopic signatures similar to that using MeOH alone. The maximum errors for EtOH and MeOH mixtures (-147.06‰ for $\delta^{18}O$ and -1104.64‰ for $\delta^{2}H$ at 1.6% MeOH and 2% EtOH) were thus comparable to the error for the highest MeOH concentration (1.6% MeOH). In contrast, MeOH caused negligible effects on IRMS values within the range of concentrations used, whereas we found larger errors for IRMS than for IRIS with EtOH concentrations starting at 4% for $\delta^{18}O$ and 1% for $\delta^{2}H$.

The post-processing correction of contaminant interference for L2110-*i* and L2120-*i* reallocated the IRIS values within threshold limits (±0.8 and ±6‰ for $\delta^{18}O$ and $\delta^{2}H$, respectively) for MeOH concentrations below 0.8% for $\delta^{18}O$ and 0.2% for $\delta^{2}H$. For EtOH, the correction always increased analytical accuracy, even though uncorrected values were usually within MAB limits (Fig. 1). The removal of organic interferences by the MCM improved the accuracy of IRIS values for both isotopes in the MeOH dilutions for contaminant concentrations up to 0.8%, but for EtOH dilutions the MCM tended to produce larger errors than the non-treated IRIS for concentrations ≥2%. In mixed dilutions, the MCM was clearly influenced by the quantity of EtOH at equal MeOH concentrations (Fig. 1). The effect of small amounts of residual MeOH after

MCM pre-treatment in the highest concentration levels was generally corrected by post-processing, but the treatment of EtOH produced overcorrected values (Fig. 1).

Effect of contaminants on water isotopic composition and correction methods: natural samples

We found significant differences in isotopic compositions between uncorrected IRIS and IRMS values for the complete set of 136 samples analysed (Table 3). The maximum discrepancies between methods were -17.25‰ ($\delta^{18}O$) and -78.08‰ ($\delta^{2}H$) for soil samples, and -8.34‰ ($\delta^{18}O$) and -92.19‰ ($\delta^{2}H$) for xylem samples. In particular, 20% ($\delta^{18}O$) and 22% ($\delta^{2}H$) of the samples fell outside the limits of the MAB, and about 10% showed very strong negative deviations (below -2‰ and -20‰, for $\delta^{18}O$ and $\delta^{2}H$, respectively, see Fig. 2a,b). After post-processing, differences in isotopic compositions between IRIS and IRMS values were still significant for $\delta^{18}O$ but became non-significant for $\delta^{2}H$ (Table 3). The maximum differences were -1.79‰ for $\delta^{18}O$ and +26.74‰ for $\delta^{2}H$ in soil samples and +1.76‰ for $\delta^{18}O$ and +8.55‰ for $\delta^{2}H$ in xylem samples. Overall, the number of samples outside the MAB decreased to 7% ($\delta^{18}O$) and 4% ($\delta^{2}H$). Deviations from IRMS values produced a slight (although within MAB limits) positive bias (Fig. 2c,d).

Considering only the subset of 79 samples reanalysed with the MCM, we also found significant differences in isotopic compositions between uncorrected IRIS and IRMS values (Table 3). Within this subset, 29% ($\delta^{18}O$) and 27% ($\delta^{2}H$) of the samples were originally outside the threshold values of the MAB. This percentage decreased to 9% ($\delta^{18}O$) and 4% ($\delta^{2}H$) after post-processing correction and to 5% ($\delta^{18}O$) and 6% ($\delta^{2}H$) with MCM pre-treatment (IRIS plus MCM, Table 2). In this regard, there were no significant differences between the pre-treatment and the software correction methods, both being statistically equivalent to IRMS. Besides, we also did not find significant differences between post-processing correction after MCM operation (IRIS plus MCM post-processed) and the other combinations (IRIS post-processed and IRIS plus MCM alone) (Table 3). However, the MCM pre-treatment produced a larger number of samples having systematic positive errors (although still within MAB limits) than the post-processing correction (Fig. 2e,f), resulting in a histogram clearly biased to positive values, particularly for $\delta^{18}O$. For the MCM with post-processing, differences in isotopic compositions between IRIS and IRMS were slightly higher than those without post-

processing, but in the range of the other two combinations, with 10% ($\delta^{18}O$) and 6% ($\delta^{2}H$) of samples outside the MAB and similar positive bias (Fig. 2g,h).

The correction based on linear regression of the water mixtures was less successful than the post-processing correction or the removal of organics by MCM. For the MeOH concentration only ('ORGANIC_MEOH_AMPL' column in the raw Picarro output files), the regression-based correction placed 13% ($\delta^{18}O$) and 26% ($\delta^{2}H$) of collected samples outside the MAB. Adding a second correction based on EtOH concentration ('ORGANIC_BASE' column) produced very similar results (data not shown).

Relationships between IRMS- and IRIS-based approaches for stable isotopes in water

Fig. 3a,b compares IRMS and IRIS values (before and after post-processing correction) for the entire dataset (N=136). Goodness-of-fit statistics (R^2 and root mean square error, RMSE) of the linear regressions between IRIS and IRMS indicated that the post-processing correction eliminated most discrepancies due to organic interference, even for highly contaminated samples.

Table 4 shows the statistics of the linear regressions between IRIS and IRMS values for the subset of samples analysed with the MCM for each category of ChemCorrect™ contamination. An important improvement in R^2 and a concomitant decrease in the RMSE were observed after activating the MCM, indicating an effective removal of interferences caused by contamination with organics. Considering the ChemCorrect™ categories, R^2 increased from 0.06 to 0.89 ($\delta^{18}O$) and from 0 to 0.88 ($\delta^{2}H$) for the red-flagged samples. For the yellow-flagged samples, R^2 increased from 0.69 to 1 ($\delta^{18}O$) and from 0.69 to 0.99 ($\delta^{2}H$). Moreover, 43 and 83% of the samples first flagged as yellow and red, respectively, were classified as green after MCM operation.

Elimination of contaminants by the MCM

We found a strong correspondence between known alcohol concentrations and ChemCorrect™ quantification values for MeOH (R^2 = 0.99) and EtOH (R^2 = 0.99). In our set of mixtures, 1% MeOH corresponded to approximately 0.1 units in the 'ORGANIC_MEOH_AMPL' column and 1% EtOH corresponded to approximately 245 units in the 'ORGANIC_BASE' column. We applied these equivalences in order to

compare the effectiveness of the MCM to remove contaminants in alcohol-water mixtures and natural samples. Mean values for equivalent MeOH and EtOH (%) concentration for each family and ChemCorrect™ flagging category are shown in Fig. 4. Equivalent MeOH concentrations in samples ranged from 0 to 0.06% for xylem water, and from 0 to 0.32% for soil samples. Equivalent EtOH concentrations ranged from 0 to 6.7% in the xylem, and from 0 to 0.03% for soil samples. These values were within the range of the set of standard dilutions (0.1-1.6% for MeOH and 0.5-8% for EtOH). MeOH was nearly completely eliminated by the MCM in both the natural samples and the set of mixtures; the estimated maximum residual concentration was 0.01% for samples and up to 0.09% for 1.6% MetOH dilutions. In contrast, the MCM was more effective at removing the EtOH from the artificial mixtures than at eliminating 'C_{2+} alcohols' in soil and xylem samples. Despite having higher initial concentrations, the residual EtOH-equivalent concentration was about one order of magnitude lower in the mixtures (mean, 0.016%; maximum, 0.03%) than in the samples (mean, 0.17%; maximum, 3.9%; see Fig. 4). The higher residual concentrations in samples, however, did not produce higher deviations from IRMS values (compare Fig.1 for artificial mixtures with Figs. 5 and 6 for the natural samples).

Contaminant effects among plant families

Figs. 5a,b,c,d and 6a,b,c,d illustrate the differences in isotopic compositions ($\delta^{18}O$ and $\delta^{2}H$, respectively) between IRIS and IRMS values (δ_{IRIS}- δ_{IRMS}) among plant families. These differences were generally negative in the most contaminated samples (see Fig. 4). Both MCM operation and post-processing correction increased the agreement between IRIS and IRMS and reallocated most samples within the established MAB threshold. The MCM, however, produced a systematic positive bias in δ_{IRIS}-δ_{IRMS} differences in almost all plant families.

DISCUSSION

A simple IRIS post-processing reduces contaminant interference

As previously reported, the isotopic composition of some natural samples analysed by IRIS showed strong negative deviations from IRMS values (Brand *et al.*, 2009; West *et al.*, 2010, 2011; Zhao *et al.*, 2011; Schmidt *et al.*, 2012). Differences were particularly high for soil samples as compared to other studies (West *et al.*, 2010; Zhao *et al.*, 2011), being in the range of previously published values for xylem samples (West *et al.*, 2010, 2011; Zhao *et al.*, 2011; Schmidt *et al.*, 2012). Nevertheless, it should be noted that the most contaminated samples (differences < -2‰ in $\delta^{18}O$) corresponded to downhill and valley-bottom soils in a gypsum-rich area, characterized by the accumulation of solutes and mineral nutrients, contrasting with the limited nutrient availability in the top of the hills (Guerrero-Campo *et al.*, 1999; Palacio *et al.*, 2014b). Hence, the potential interference of electrolytes in soils with IRIS measurements may require a more detailed assessment.

The post-processing correction proposed by Picarro strongly reduced the effects of contamination, even in cases of heavily contaminated samples. As expected, the correction limits for MeOH were relatively low due to its strong spectral interference (deviations were within MAB up to concentrations of 0.4% and 0.1% MetOH for $\delta^{18}O$ and $\delta^{2}H$, respectively). Conversely, the deviation of corrected values was below the MAB even at the highest tested concentration of EtOH (8%). For xylem and soil samples, the post-processing correction reduced the discrepancies between IRIS and IRMS from RMSEs of 2.42‰ to 0.42‰ for $\delta^{18}O$ and of 18.46‰ to 3.95‰ for $\delta^{2}H$, and reallocated more than 70% of highly deviating samples within MAB limits. Nevertheless, a closer look at the error distribution (Fig. 2c,d) reveals a positive error bias of about 0.2‰ for $\delta^{18}O$ and 2‰ for $\delta^{2}H$. This bias, however, is in the range of the expected additive effect of laboratory uncertainties and potential sample alteration during transport and storage. In fact, we also found slightly positive differences between IRIS and IRMS for the pure water samples used for the set of alcohol-water mixtures (up to +0.36‰ for $\delta^{18}O$, and +0.89‰ for $\delta^{2}H$, see Fig. 1). In this regard, our results show the potential of post-processing correction methods as a way to solve contaminant issues for IRIS, but also encourage a more exhaustive assessment of their accuracy, e.g. following the robust procedures of global inter-laboratory tests.

MCM: effectiveness and limitations

An overall reduction in the maximum differences between IRIS and IRMS values in the natural samples was obtained with the MCM in operation, even for highly contaminated samples. The RMSE decreased to 0.54‰ for $\delta^{18}O$ and 3.52‰ for $\delta^{2}H$. More than 75% of samples initially placed outside the MAB fell within this threshold after using the MCM. The post-processing correction and the MCM were generally equally effective for $\delta^{18}O$ analysis in the presence of MeOH contamination, but the post-processing correction was less precise for $\delta^{2}H$ (Table 4). Indeed, when methanol was the main contaminant (as in methanol-water mixtures and in contaminated soil samples; Fig. 4a), MCM seemed to outperform the post-processing correction (Fig. 1, Fig. 5b,c, and Fig. 6b,c). In contrast, the post-processing correction was consistently more effective than the MCM at removing errors associated with C_{2+} alcohols such as EtOH (see Fig. 1). Furthermore, using the MCM a substantial proportion of samples showed positive deviations between 0.4‰ and 0.8‰ for $\delta^{18}O$, and between 2‰ and 6‰ for $\delta^{2}H$ (Fig. 2e,f). This positive bias is likely to be a collateral effect of the contaminant removal. MCM oxidation converts organic compounds into CO_2 and nascent water by using an air carrier gas supported by ambient O_2. For each EtOH molecule, the MCM generates three water molecules that mix with the water in the sample. In this reaction the hydrogen atoms originate from the alcohol, whereas the oxygen mostly comes from the carrier gas ($\delta^{18}O_{air}$ = +23.8 ± 0.3‰ (Coplen *et al.*, 2002)). If the alcohol content in the sample is sizeable, the MCM significantly alters the isotopic signature of the water proportionally to (i) the relative mass contribution of the hydrogen and oxygen atoms of the sample water and that of the water formed through chemical oxidation of alcohols, and (ii) their corresponding isotopic signatures. Our results were consistent with this expectation, with more biased values for $\delta^{18}O$ than for $\delta^{2}H$ analysed by the MCM in comparison to IRMS, due to the very positive oxygen isotopic composition of air. Large errors can consequently be generated at high concentrations of organic contaminants in the samples because the oxidation process adds new water molecules to the water pool, despite effectively reducing spectral interference. We would thus recommend post-processing correction instead of MCM operation when analysing samples of unknown composition or with expectedly high concentrations of EtOH and longer-chain alcohols.

The MCM nearly completely eliminated MeOH and EtOH from the artificial mixtures, but was less effective at removing the C_{2+} alcohols pool from natural samples

(presumably including ethanol derived from anaerobic metabolism, terpenols and other volatiles, see refs. in (Niinemets U. and Monson R.K. (eds.), 2013). Despite this, the artificial mixtures still produced divergences beyond the MAB for concentrations above 0.4% MeOH and 2% EtOH, due to the side-effects of the oxidation process. Conversely, we could not establish a clear threshold for natural samples based on estimated contaminant concentration (Fig. 4). Although the concentrations of C_{2+} alcohols remaining after MCM operation were higher in the natural samples than in the mixtures, the spectral interference was significantly lower in the samples. This could be attributed to a limited interference of other C_{2+} alcohols as compared to EtOH.

We also tested the possibility of applying post-processing correction to samples previously treated by micro-combustion to improve the performance of the MCM. The post-processing correction, however, apparently overcorrected the isotopic values, with the exception of highly contaminated samples with residual MeOH (see Fig. 2g,h). The MCM was designed to remove the spectral interference of organic compounds at low concentrations. In samples with high concentrations of contaminants (e.g. EtOH dilutions) the organic interference is effectively removed by the MCM, but at the expense of altering the isotope composition of water. Hence, although post-processing may still correct the spectral interferences caused by remaining alcohols after MCM operation, the resulting "corrected" values will be those of the isotopically-altered water. The development of an integrated post-processing correction would thus be advisable (e.g. considering spectral information before and after MCM operation) as a way to account for changes in water isotope composition caused by the MCM.

Spectral post-processing outperforms previously proposed empirical corrections

Previous studies have proposed correction curves as a function of the degree of contaminant concentration (Brand *et al.*, 2009; Schultz *et al.*, 2011; Leen *et al.*, 2012). Schultz *et al.* (2011) eliminated (for $\delta^{18}O$) or reduced (for $\delta^{2}H$) the discrepancies between IRIS and IRMS results using an LGR Liquid Water Isotope Analyzer (Los Gatos Research Inc., Mountain View, CA). The recommended curves, however, did not match those provided by the manufacturer, so the authors suggested that every analyser could require a customized correction. Brand *et al*. (2009) also performed regressions of δ-values and contaminant concentrations for a set of standard dilutions and concluded that corrections of isotopic values are feasible provided the alcohol content in the samples is known. We consequently corrected the isotopic values by using linear

regressions to predict IRIS δ-errors for pure water as a function of contaminant concentration according to the CH_3OH and C_{2+} alcohol outputs from ChemCorrect™. The precision however, was lower than that obtained through post-processing correction, and the most contaminated samples were usually extremely overcorrected, resulting in very high isotopic values. Post-processing correction based on peaks filtered by ChemCorrect™ seems thus a more suitable alternative than the correction based on organic concentrations in samples.

In spite of this, corrections based on estimated MeOH concentrations still improved the accuracy of isotopic records, but the calibrations performed with the EtOH dilutions did not work well for natural samples. This could be due to the fact that MeOH concentration can be specifically quantified based on a well-defined peak, whereas EtOH produces mainly a baseline drift in the spectra, and is measured together with a pool of long-chain alcohols. Similarly, Brand *et al*. (2009) found no relationship between EtOH concentration and δ-value in wine due to interference from contaminants such as MeOH, phenols, or organic acids.

Concluding remarks

According to our results, the post-processing correction of isotope values based on spectral analyses improves significantly the performance of IRIS in soil and xylem samples, thus allowing detailed ecohydrological studies at a reasonable cost. In particular, differences between IRMS and IRIS-corrected values fell within reasonable limits in most field-collected samples (>90%). According to our dilution tests, interferences associated to organic contaminants can be successfully removed with concentrations up to 8% and 0.4% for EtOH and MeOH, respectively. Sample pre-treatment through the MCM slightly outperforms post-processing correction in removing MeOH interference. Nevertheless, for heavily MeOH-contaminated samples, the best results would be obtained combining both methods, which together may be able to correct samples with up to 1.6% MeOH contamination. In contrast, the MCM was not effective in removing EtOH interference: with high concentrations of contaminant the module causes significant changes in the isotope composition of water (particularly strong for $\delta^{18}O$). Hence, for contaminated samples we generally recommend to adopt post-processing correction in isotopic analyses, and only when the main (and mostly

559 unique) contaminant detected is MeOH (as in our soil samples), the use of MCM
560 (eventually combined with post-processing correction).
561
562 **ACKNOWLEDGMENTS**

563 This research was supported by the Spanish Government projects CGL2013-48074-P,
564 AGL 2012-40039-C02 and AGL 2012-40151-C03, the Catalan Government project
565 SGR 2014-274 and the European Research Council Synergy grant ERC- 2013-SyG-
566 610028 IMBALANCE-P. The Spanish Government funded the FPU predoctoral
567 fellowship to P.M., the FPI predoctoral fellowship and travel grant to A.B., and the
568 Ramón y Cajal Programme to J.P.F. (RYC-2008-02050). We thank Gregor Hsiao for
569 sharing the post-processing correction, and for his useful advice. We thank Pilar
570 Sopeña, Mireia Oromí, Paul Brooks, Rolf Siegwolf and Matthias Saurer for their
571 technical support with isotope analyses. We also thank the useful comments from
572 Margaret Barbour and three anonymous referees, who made a substantial contribution to
573 the revised manuscript.
574

REFERENCES

Berman ESF, Gupta M, Gabrielli C, Garland T, McDonnell JJ. **2009**. High-frequency field-deployable isotope analyzer for hydrological applications. *Water Resources Research* **45**: n/a–n/a.

Brand WA, Geilmann H, Crosson E, Rella C. **2009**. Cavity ring-down spectroscopy versus high-temperature conversion isotope ratio mass spectrometry; a case study on δ^2H and $\delta^{18}O$ of pure water samples and alcohol/water mixtures. *Rapid Communications in Mass Spectrometry* **23**: 1879–1884.

Coplen TB, Bohlke JK, De Bievre P, Ding T, Holden NE, Hopple JA, Krouse HR, Lamberty A, Peiser HS, Revesz K, *et al.* 2002. Isotope-abundance variations of selected elements (IUPAC Technical Report). *Pure and Applied Chemistry* **74**: 1987–2017.

Dawson TE. **1996**. Determining water use by trees and forests from isotopic, energy balance and transpiration analyses: the roles of tree size and hydraulic lift. *Tree physiology* **16**: 263–272.

Dawson TE, Ehleringer JR. **1993**. Isotopic enrichment of water in the "woody" tissues of plants: Implications for plant water source, water uptake, and other studies which use the stable isotopic composition of cellulose. *Geochimica Et Cosmochimica Acta* **57**: 3487–3492.

Dawson TE, Simonin KA. **2011**. The roles of stable isotopes in forest hydrology and biogeochemistry: synthesis of research and future directions. In: Levis D, Carlyle-Moses D, Tanaka T, eds. *Forest Hydrology and Biogeochemistry*. Springer Netherlands, 137–161.

Ehleringer JR, Dawson TE. **1992**. Water uptake by plants: perspectives from stable isotope composition. *Plant, Cell and Environment* **15**: 1073–1082.

Goldsmith GR, Muñoz-Villers LE, Holwerda F, Mcdonnell JJ, Asbjornsen H, Dawson TE. **2012**. Stable isotopes reveal linkages among ecohydrological processes in a seasonally dry tropical montane cloud forest. *Ecohydrology* **5**: 779–790.

Guerrero-Campo J, Alberto F, Hodgson J, García-Ruiz JM, Montserrat-Martí G. **1999**. Plant community patterns in a gypsum area of NE Spain. I. Interactions with topographic factors and soil erosion. *Journal of Arid Environments* **41**: 401–410.

Gupta P, Noone D, Galewsky J, Sweeney C, Vaughn BH. **2009**. Demonstration of high-precision continuous measurements of water vapor isotopologues in laboratory and remote field deployments using wavelength-scanned cavity ring-down spectroscopy (WS-CRDS) technology. *Rapid Communications in Mass Spectometry* **23**: 2534–2542.

Johnson LR, Sharp ZD, Galewsky J, Strong M, Van Pelt AD, Dong F, Noone D. **2011**. Hydrogen isotope correction for laser instrument measurement bias at low water vapor concentration using conventional isotope analyses: application to measurements

from Mauna Loa Observatory, Hawaii. *Rapid Communications in Mass Spectrometry* **25**: 608–616.

Leen JB, Berman ESF, Liebson L, Gupta M. **2012**. Spectral contaminant identifier for off-axis integrated cavity output spectroscopy measurements of liquid water isotopes. *Review of Scientific Instruments* **83**.

Lilleskov EA, Bruns TD, Dawson TE, Camacho FJ. **2009**. Water sources and controls on water-loss rates of epigeous ectomycorrhizal fungal sporocarps during summer drought. *New Phytologist* **182**: 483–494.

Lis G, Wassenaar LI, Hendry MJ. **2008**. High-precision laser spectroscopy D/H and $^{18}O/^{16}O$ measurements of microliter natural water samples. *Analytical chemistry* **80**: 287–293.

Moreno-Gutiérrez C, Dawson TE, Nicolás E, Querejeta JI. **2012**. Isotopes reveal contrasting water use strategies among coexisting plant species in a mediterranean ecosystem. *New Phytologist* **196**: 489–496.

Niinemets U. and Monson R.K. (eds.). **2013**. *Biology, Controls and Models of Tree Volatile Organic Compound Emissions*. Springer ScienceBusiness.

Palacio S, Azorín J, Montserrat-Martí G, Ferrio JP. **2014a**. The crystallization water of gypsum rocks is a relevant water source for plants. *Nature communications* **5**: 4660.

Palacio S, Maestro M, Montserrat-Martí G. **2014b**. Differential nitrogen cycling in semiarid sub-shrubs with contrasting leaf habit. *PLoS ONE* **9**: e93184.

Picarro. **2010**. ChemCorrect™ - Solving the Problem of Chemical Contaminants in H_2O Stable Isotope Research. *White paper*: 2–4.

Picarro. **2012**. Micro-Combustion Module™ (MCM): Elimination of Organics Datasheet.

Prieto I, Armas C, Pugnaire FI. **2012**. Water release through plant roots: New insights into its consequences at the plant and ecosystem level. *New Phytologist* **193**: 830–841.

Richman BA, Hsiao GS, Rella C. **2010**. Detecting and Eliminating Interfering Organic Compounds in Waters Analyzed for Isotopic Composition by CRDS. *AGU Fall Meeting Abstracts* **1**: 0379.

Saad N, Hsiao G, Chapellet-Volpini L, Vu D. **2013**. Two-pronged approach to overcome spectroscopically interfering organic compounds with isotopic water analysis. *EGU General Assembly Conference Abstracts* **15**: 13296.

Schmidt M, Maseyk K, Lett C, Biron P, Richard P, Bariac T, Seibt U. **2012**. Reducing and correcting for contamination of ecosystem water stable isotopes measured by isotope ratio infrared spectroscopy. *Rapid Communications in Mass Spectrometry* **26**: 141–153.

649 **Schultz NM, Griffis TJ, Lee X, Baker JM**. **2011**. Identification and correction of
650 spectral contamination in $^{2}H/^{1}H$ and $^{18}O/^{16}O$ measured in leaf, stem, and soil water.
651 *Rapid Communications in Mass Spectrometry* **25**: 3360–3368.

652 **Treydte K, Boda S, Graf Pannatier E, Fonti P, Frank D, Ullrich B, Saurer M,**
653 **Siegwolf R, Battipaglia G, Werner W, *et al.* 2014**. Seasonal transfer of oxygen
654 isotopes from precipitation and soil to the tree ring: Source water versus needle water
655 enrichment. *New Phytologist* **202**: 772–783.

656 **Warren JM, Brooks JR, Meinzer FC, Eberhart JL**. **2008**. Hydraulic redistribution of
657 water from *Pinus ponderosa* trees to seedlings: Evidence for an ectomycorrhizal
658 pathway. *New Phytologist* **178**: 382–394.

659 **Wassenaar LI, Ahmad M, Aggarwal P, van Duren M, Pöltenstein L, Araguas L,**
660 **Kurttas T**. **2012**. Worldwide proficiency test for routine analysis of $\delta^{2}H$ and $\delta^{18}O$ in
661 water by isotope-ratio mass spectrometry and laser absorption spectroscopy. *Rapid*
662 *communications in mass spectrometry* **26**: 1641–8.

663 **Wassenaar LI, Coplen TB, Aggarwal PK**. **2014**. Approaches for achieving long-term
664 accuracy and precision of $\delta^{18}O$ and $\delta^{2}H$ for waters analyzed using laser absorption
665 spectrometers. *Environmental Science and Technology* **48**: 1123–1131.

666 **West A, Goldsmith G, Brooks P, Dawson T**. **2010**. Discrepancies between isotope
667 ratio infrared spectroscopy and isotope ratio mass spectrometry for the stable isotope
668 analysis of plant and soil waters. *Rapid Communications in Mass Spectometry* **24**:
669 1948–1954.

670 **West AG, Goldsmith GR, Matimati I, Dawson TE**. **2011**. Spectral analysis software
671 improves confidence in plant and soil water stable isotope analyses performed by
672 isotope ratio infrared spectroscopy (IRIS). *Rapid Communications in Mass*
673 *Spectrometry* **25**: 2268–2274.

674 **Zhao L, Xiao H, Zhou J, Wang L, Cheng G, Zhou M, Yin L, McCabe MF**. **2011**.
675 Detailed assessment of isotope ratio infrared spectroscopy and isotope ratio mass
676 spectrometry for the stable isotope analysis of plant and soil waters. *Rapid*
677 *Communications in Mass Spectrometry* **25**: 3071–3082.

678

679 **FIGURE LEGENDS**

680

681 **Fig. 1** Errors for $\delta^{18}O$ and $\delta^{2}H$ (‰) associated with various methanol (MeOH) and
682 ethanol (EtOH) concentrations in the alcohol-water mixtures. The errors have been
683 calculated as the differences between the dilutions and pure water analysed by IRMS.
684 Dashed lines represent the accuracy thresholds based on the maximum accepted bias
685 (MAB) established by the International Agency of Atomic Energy.

686

687 **Fig. 2** Histogram representing the distribution of deviations between IRIS and IRMS for
688 $\delta^{18}O$ (left panels) and $\delta^{2}H$ (right panels). (a,b) IRIS uncorrected; (c,d) IRIS post-
689 processed; (e,f) IRIS plus MCM; (g,h) IRIS plus MCM plus post-processing. The
690 samples were grouped into 0.2‰ and 2‰ intervals, for $\delta^{18}O$ and $\delta^{2}H$, respectively. For
691 simplicity, heavily deviated samples (outside the [-2‰ +2‰] range for $\delta^{18}O$ and the [-
692 20‰ +20‰] range for $\delta^{2}H$) were included in a single bin. Light grey: whole dataset.
693 Dark grey: subsample used for the assessment of the MCM.

694

695 **Fig. 3** Comparison between IRIS and IRMS for uncorrected (filled symbols) and post-
696 processed (empty symbols) $\delta^{18}O$ values (a) and $\delta^{2}H$ values (b) using 136 field samples.
697 Linear regression equations, R^2 and RMSEs are also presented. Dotted lines represent
698 95% confidence intervals. Circles, xylem samples; Triangles, soil samples.

699

700 **Fig. 4** Estimated equivalent concentrations (%) of methanol (MeOH, upper panels) and
701 ethanol (EtOH, lower panels) by plant family, determined by fitting the spectral
702 information provided by the Chemcorrect™ (respectively, 'ORGANIC_MEOH_AMPL'
703 and 'ORGANIC_BASE' columns in the raw output files) against known values of
704 MeOH and EtOH in the alcohol-water mixtures. Within each family, three coloured bars
705 indicate the flagging categories of ChemCorrect™. Left and right panels show raw
706 sample concentrations and concentrations after MCM pre-treatment, respectively.

707

708 **Fig. 5** Differences in $\delta^{18}O$ values between IRIS and IRMS by plant family. IRIS
709 uncorrected (a), IRIS post-processed (b), IRIS plus MCM (c) and IRIS plus MCM plus
710 post-processing (d). Error bars are standard errors. Dashed lines identify the maximum

711 accepted bias (MAB) established by the International Agency of Atomic Energy.
712 Colour codes represent the flagging categories of ChemCorrect™.
713
714 **Fig. 6** Differences in δ^2H values between IRIS and IRMS by plant family. IRIS
715 uncorrected (a), IRIS post-processed (b), IRIS plus MCM (c) and IRIS plus MCM plus
716 post-processing (d). Error bars are standard errors. Dashed lines identify the maximum
717 accepted bias (MAB) established by the International Agency of Atomic Energy.
718 Colour codes represent the flagging categories of ChemCorrect™.
719

720 **Table 1.** Description of the plant species and soil samples used in this study. Soil
721 description according to FAO classification.

Species/Soil type	Family	Season	Origin	No. of samples	No. of samples in the MCM subset
Arbutus unedo L.	Ericaceae	Fall, winter & summer	Catalonia	5	3
Artemisia herba-alba Asso	Asteraceae	Spring	Aragon	1	1
Baccharis pilularis DC.	Asteraceae	Fall	California	7	5
Buxus sempervirens L.	Buxaceae	Summer	Aragon	3	3
Cistus clusii Dunal	Cistaceae	Fall	Murcia	3	0
Erica arborea L.	Ericaceae	Winter & summer	Catalonia	4	2
Erica multiflora L.	Ericaceae	Fall, winter & summer	Valencia	5	1
Fagus sylvatica L.	Fagaceae	Summer	Catalonia	1	1
Helianthemum squamatum (L.) Dum. Cours.	Cistaceae	Spring	Aragon	4	4
Lepidium subulatum L.	Brassicaceae	Spring	Aragon	3	3
Linum suffruticosum L.	Linaceae	Spring	Aragon	1	1
Stipa tenacissima L.	Poaceae	Fall & spring	Andalusia	3	2
Phillyrea latifolia L.	Oleaceae	Fall, winter & summer	Catalonia	4	1
Phlomis purpurea sub. *almeriensis* Pau	Lamiaceae	Fall	Andalusia	2	0
Pinus halepensis Mill.	Pinaceae	Fall	Murcia	2	0
Pinus sylvestris L.	Pinaceae	Summer	Aragon	4	4
Pistacia lentiscus L.	Chenopodiaceae	Winter	Catalonia	2	1
Quercus agrifolia Née	Fagaceae	Fall	California	3	3
Quercus coccifera L.	Fagaceae	Winter	Catalonia	1	0
Quercus douglasii Hook. & Arn.	Fagaceae	Fall	California	3	1
Quercus ilex L.	Fagaceae	All	Catalonia	13	6
Quercus kelloggii Newb.	Fagaceae	Fall	California	9	6
Quercus lobata Née	Fagaceae	Fall	California	14	7
Quercus subpyrenaica Villar	Fagaceae	Summer	Aragon	4	4
Suaeda pruinosa Lange	Chenopodiaceae	Spring	Aragon	1	1
Umbellularia californica Hook. & Arn.	Lauraceae	Fall	California	5	4
TOTAL xylem				**107**	**64**
Calcaric Leptosol		Winter & summer	Catalonia	5	3
Calcic Cambisol		Summer	Aragon	2	2
Dystric Cambisol		Spring	Catalonia	5	0
Dystric Leptosol		Spring & summer	Catalonia	7	0
Gypsiric Regosol		Spring	Aragon	4	4
Gypsisol/Solonchak		Spring	Aragon	6	6
TOTAL soil				**29**	**15**
TOTAL				136	79

722

723 **Table 2.** Range (minimum value; maximum value) of $\delta^{18}O$ and $\delta^{2}H$ discrepancies between IRIS and IRMS, and number of samples within the
724 maximum accepted bias (MAB) used in the last proficiency test of the International Atomic Energy Agency (±0.8‰ for $\delta^{18}O$ and ±6‰ for $\delta^{2}H$,
725 IAEA-TEL-2011-01, see text for details) for IRIS, IRIS plus post-processing correction, and IRIS plus the MCM (either uncorrected or post-
726 processed) in standard dilutions and the subset (*N*=79) of xylem and soil water samples.

IRIS									
		Uncorrected				Post-processed			
Sample type	No. total samples	Error $\delta^{18}O$ (‰)	No. within MAB	Error $\delta^{2}H$ (‰)	No. within MAB	Error $\delta^{18}O$ (‰)	No. within MAB	Error $\delta^{2}H$ (‰)	No. within MAB
Standard dilutions									
MeOH	5	(-142.96; -8.64)	0	(-1077.00; -64.58)	0	(-2.15; -0.01)	3	(3.35; 44.39)	1
EtOH	5	(-0.39; 0.20)	5	(-10.76; 0.49)	4	(0.13; 0.46)	5	(-4.38; 0.56)	5
MeOH+EtOH	4	(-147.06; -39.65)	0	(-1104.64; -298.72)	0	(-2.29; -0.38)	2	(6.98; 45.39)	0
Collected samples									
Xylem	64	(-8.34; 0.85)	48	(-92.19; 6.17)	50	(-0.33; 1.43)	60	(-1.01; 8.55)	62
Soil	15	(-17.25; 0.24)	8	(-78.08; 4.99)	8	(-1.79; 0.49)	12	(0.13; 6.66)	14
IRIS plus MCM									
		Uncorrected				Post-processed			
Sample type	No. total samples	Error $\delta^{18}O$ (‰)	No. within MAB	Error $\delta^{2}H$ (‰)	No. within MAB	Error $\delta^{18}O$ (‰)	No. within MAB	Error $\delta^{2}H$ (‰)	No. within MAB
Standard dilutions									
MeOH	5	(-8.61; 0.41)	3	(-77.01; 1.21)	3	(0.31; 0.90)	4	(-2.96; 1.90)	5
EtOH	5	(0.22; 2.08)	3	(-19.45; -0.59)	3	(0.41; 2.48)	3	(-17.24; -0.07)	3
MeOH+EtOH	4	(0.31; 2.44)	2	(-23.08; -10.27)	0	(1.11; 3.08)	0	(-19.38; -4.64)	1
Collected samples									
Xylem	64	(-0.92; 1.21)	60	(-8.97; 8.78)	60	(0.01; 1.36)	56	(0.57; 8.91)	60
Soil	15	(-0.09; 0.79)	15	(0.16; 6.5)	14	(-0.09; 0.8)	15	(0.4; 7.45)	14

Table 3. *P*-values and *F*-ratio of the statistical comparisons (α = 0.05, mixed models based on Restricted Maximum Likelihood, REML) between correction methods for the complete dataset (*N* = 136) and a subset of natural samples (*N* = 79) for both $\delta^{18}O$ and $\delta^{2}H$.

		$\delta^{18}O$		$\delta^{2}H$	
		F-ratio	*P*-value	*F*-ratio	*P*-value
Complete dataset *N*=136	IRMS vs. IRIS uncorrected	9.6875	0.0061*	4.5324	0.0390 *
	IRIS post-processed vs. IRIS uncorrected	29.4845	<0.0001*	8.2688	0.0062 *
	IRMS vs. IRIS post-processed	5.3707	0.0327 *	0.5574	0.4593
Subset *N*=79	IRMS vs. IRIS uncorrected	4.2368	0.0443 *	4.7005	0.0341 *
	IRIS post-processed vs. IRIS uncorrected	6.6844	0.0124 *	8.3796	0.0053 *
	IRIS+MCM vs. IRIS uncorrected	8.7293	0.0046 *	8.0996	0.0060 *
	IRMS vs. IRIS post-processed	0.2778	0.6002	0.5281	0.4702
	IRMS vs. IRIS+MCM	0.8032	0.374	0.4596	0.5004
	IRIS post-processed vs. IRIS+MCM	0.1363	0.7134	0.0024	0.9613
	IRIS+MCM vs. IRIS+MCM post-processed	0.1213	0.7289	0.1488	0.7010

Table 4. Summary statistics of the relationship between IRMS and IRIS values for the subset of natural samples analysed with the MCM (N=79) within each ChemCorrect™ contamination categories. N, Number of samples, R^2 coefficient of determination for the linear regression between IRIS and IRMS, RMSE (‰); Root mean square error of the difference between IRMS and IRIS values.

	ChemCorrect Category	Green			Yellow			Red			All		
	IRMS-IRIS Linear regression	N	R^2	RMSE	N	R^2	RMSE	N	R^2	RMSE	N	R^2	RMSE
$\delta^{18}O$	IRIS	37	0.97	0.53	13	0.69	1.43	29	0.06	5.09	79	0.31	3.16
	IRIS post-processed		0.99	0.27		0.97	0.54		0.92	0.56		0.97	0.44
	IRIS+MCM	56	0.99	0.54	11	1.00	0.58	12	0.89	0.50	79	0.98	0.54
	IRIS+MCM post-processed		0.99	0.58		1.00	0.62		0.98	0.75		0.99	0.62
$\delta^{2}H$	IRIS	37	0.89	3.33	13	0.69	5.87	29	0.00	38.34	79	0.05	23.46
	IRIS post-processed		0.98	2.45		0.96	2.50		0.95	3.60		0.96	2.93
	IRIS+MCM	56	0.97	3.55	11	0.99	2.62	12	0.88	4.05	79	0.93	3.52
	IRIS+MCM post-processed		0.97	4.00		0.98	3.06		0.99	3.55		0.97	3.82

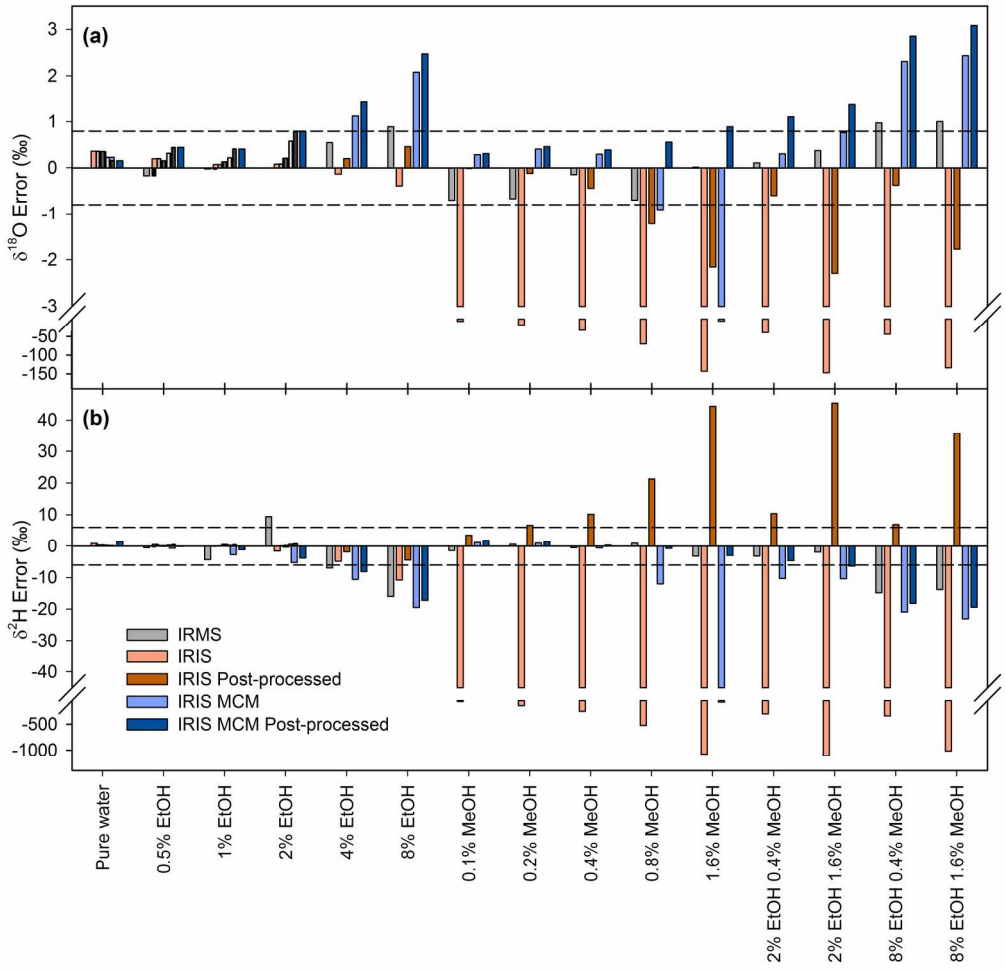

Fig. 1 Errors for $\delta^{18}O$ and $\delta^{2}H$ (‰) associated with various methanol (MeOH) and ethanol (EtOH) concentrations in the alcohol-water mixtures. The errors have been calculated as the differences between the dilutions and pure water analysed by IRMS. Dashed lines represent the accuracy thresholds based on the maximum accepted bias (MAB) established by the International Agency of Atomic Energy.
189x182mm (300 x 300 DPI)

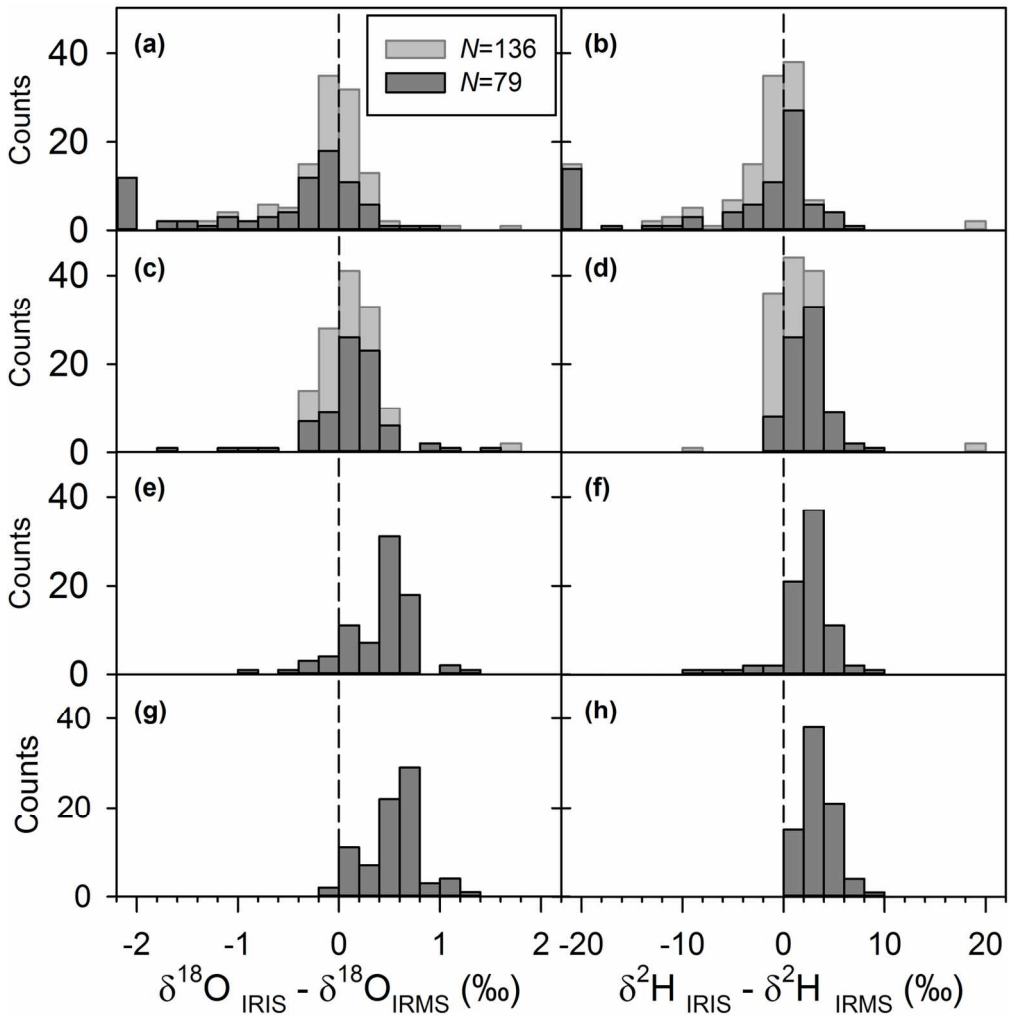

Fig. 2 Histogram representing the distribution of deviations between IRIS and IRMS for $\delta^{18}O$ (left panels) and $\delta^{2}H$ (right panels). (a,b) IRIS uncorrected; (c,d) IRIS post-processed; (e,f) IRIS plus MCM; (g,h) IRIS plus MCM plus post-processing. The samples were grouped into 0.2‰ and 2‰ intervals, for $\delta^{18}O$ and $\delta^{2}H$, respectively. For simplicity, heavily deviated samples (outside the [-2‰ +2‰] range for $\delta^{18}O$ and the [-20‰ +20‰] range for $\delta^{2}H$) were included in a single bin. Light grey: whole dataset. Dark grey: subsample used for the assessment of the MCM.
136x138mm (300 x 300 DPI)

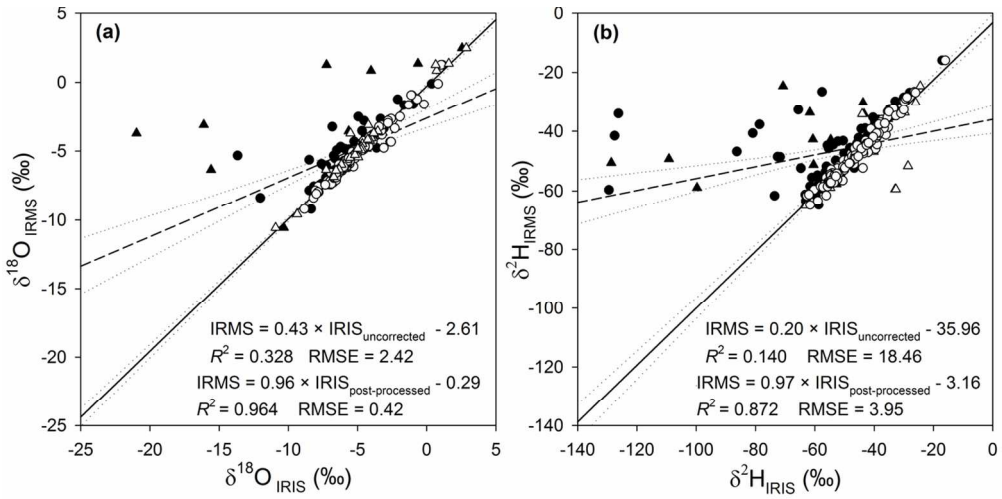

Fig. 3 Comparison between IRIS and IRMS for uncorrected (filled symbols) and post-processed (empty symbols) $\delta^{18}O$ values (a) and $\delta^{2}H$ values (b) using 136 field samples. Linear regression equations, R^2 and RMSEs are also presented. Dotted lines represent 95% confidence intervals. Circles, xylem samples; Triangles, soil samples.
118x58mm (300 x 300 DPI)

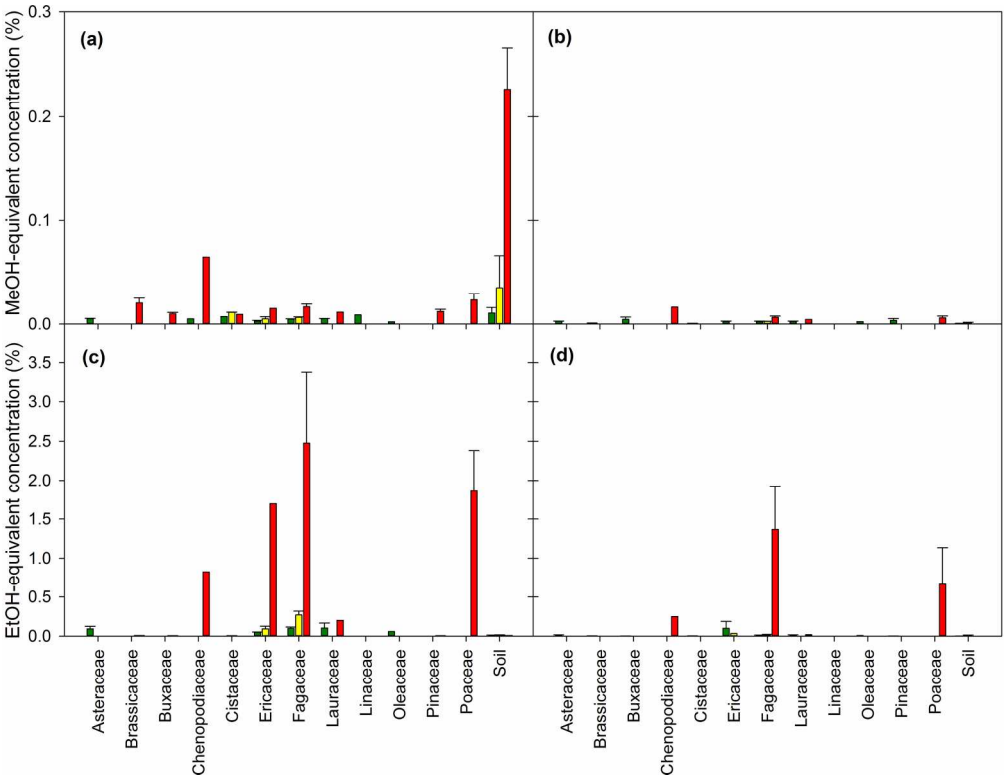

Fig. 4 Estimated equivalent concentrations (%) of methanol (MeOH, upper panels) and ethanol (EtOH, lower panels) by plant family, determined by fitting the spectral information provided by the ChemcorrectTM (respectively, 'ORGANIC_MEOH_AMPL' and 'ORGANIC_BASE' columns in the raw output files) against known values of MeOH and EtOH in the alcohol-water mixtures. Within each family, three coloured bars indicate the flagging categories of ChemCorrect™. Left and right panels show raw sample concentrations and concentrations after MCM pre-treatment, respectively.
196x151mm (300 x 300 DPI)

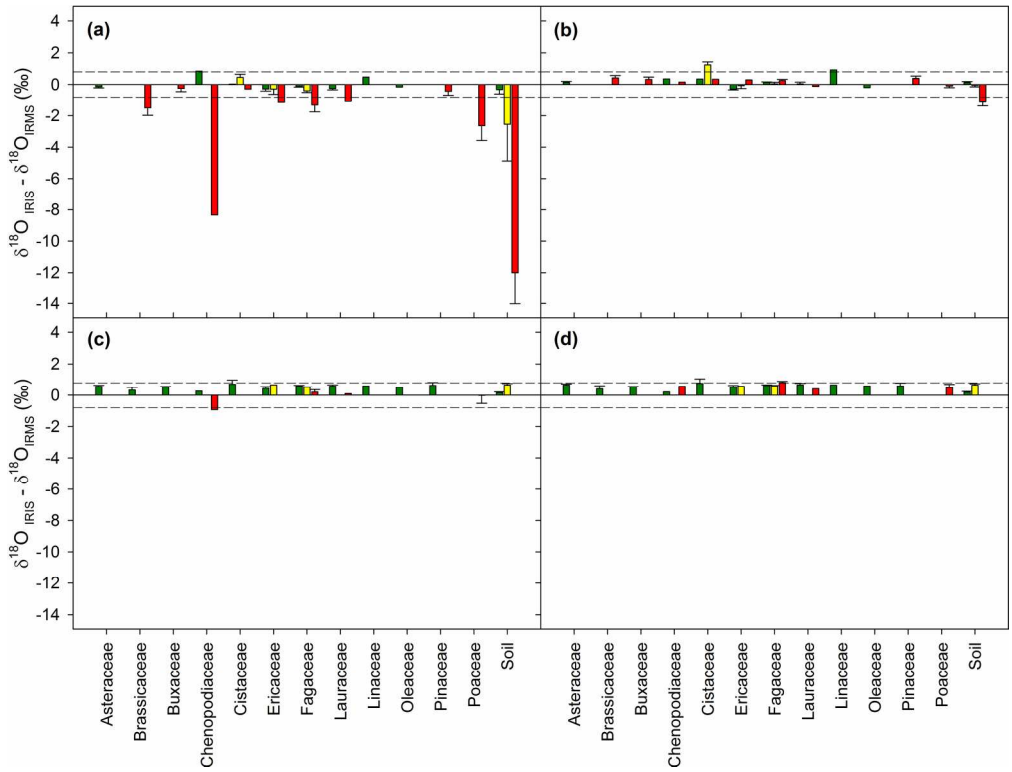

Fig. 5 Differences in $\delta^{18}O$ values between IRIS and IRMS by plant family. IRIS uncorrected (a), IRIS post-processed (b), IRIS plus MCM (c) and IRIS plus MCM plus post-processing (d). Error bars are standard errors. Dashed lines identify the maximum accepted bias (MAB) established by the International Agency of Atomic Energy. Colour codes represent the flagging categories of ChemCorrect™.
195x148mm (300 x 300 DPI)

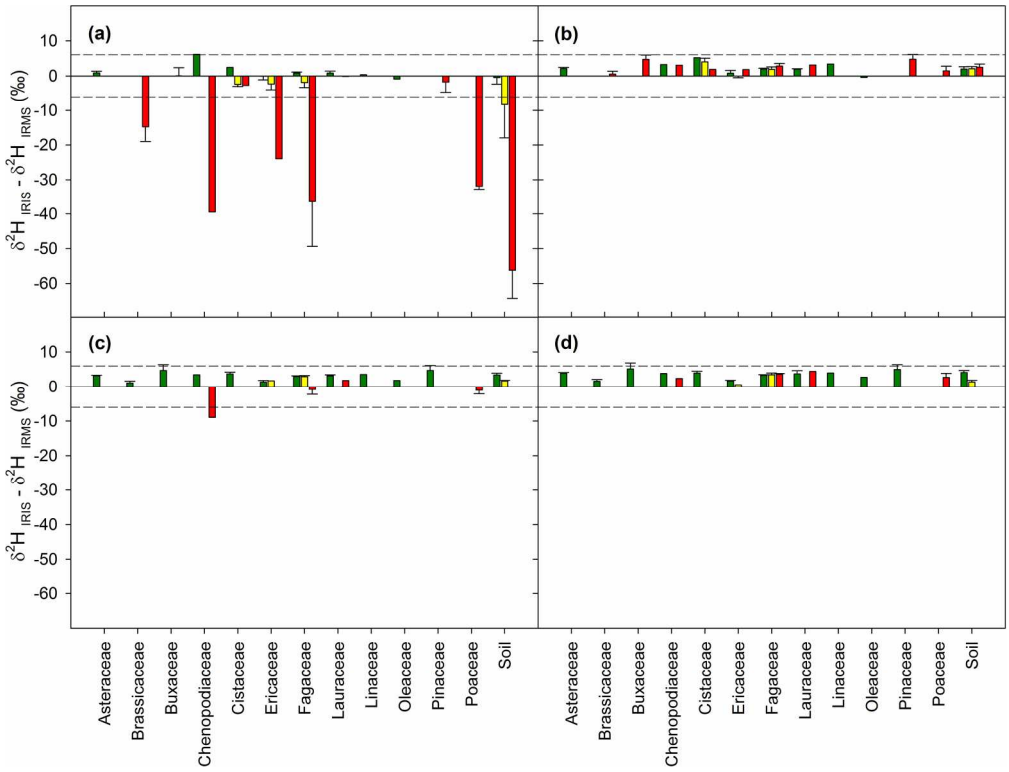

Fig. 6 Differences in δ^2H values between IRIS and IRMS by plant family. IRIS uncorrected (a), IRIS post-processed (b), IRIS plus MCM (c) and IRIS plus MCM plus post-processing (d). Error bars are standard errors. Dashed lines identify the maximum accepted bias (MAB) established by the International Agency of Atomic Energy. Colour codes represent the flagging categories of ChemCorrect™.
195x148mm (300 x 300 DPI)